Acta Geologica Polonica, Vol. 54 (2004), No. 1, pp. 61-76

Tectonic origin of the unique Holocene travertine from the Holy Cross Mts.: microbially and abiologically mediated calcium carbonate, and manganese oxide precipitation

MICHAŁ GRUSZCZYŃSKI[1,2], BOLESŁAW J. KOWALSKI[1], ROBERT SOŁTYSIK[1] & HELENA HERCMAN[3]

[1]*Wydział Matematyczno-Przyrodniczy, Instytut Geografii, Akademia Świętokrzyska, ul. Świętokrzyska 15, 25-406 Kielce, Poland*
[2]*Instytut Paleobiologii, Polska Akademia Nauk, ul. Twarda 51/55, 00-818 Warszawa, Poland*
[3]*Instytut Nauk Geologicznych, Polska Akademia Nauk, ul. Twarda 51/55, 00-818 Warszawa, Poland*

ABSTRACT:

GRUSZCZYŃSKI, M., KOWALSKI, B.J., SOŁTYSIK, R. & HERCMAN, H. 2004. Tectonic origin of the unique Holocene travertine from the Holy Cross Mts.: microbially and abiologically mediated calcium carbonate and manganese oxide precipitation. *Acta Geologica Polonica*, **54**, (1), 61-76. Warszawa.

Recent tectonic activity of the main dislocation within the Palaeozoic core of the Holy Cross Mts. led to formation of a large travertine dome of Holocene age. The main body of the travertine is built up of extremely fast crystallized calcite from highly supersaturated solutions derived from hydrothermal waters circulating through the tectonic dislocation. Many calcite crystals display the remains of calcified bacilliform bacteria rods suggesting an essential part, of the calcite crystallization process was on a bacterial precursor. Successively, after the micrite calcite travertine frame had been formed, almost pure monoclinic manganese oxide (α-MnO_2) precipitated filling part of the remaining porosity. The unique characteristics of manganese oxide crystallization also suggest a very fast process of manganese oxidation due to increase in Eh and the activity of abundant fungal species which might be associated with a specific symbiotic bacterium. Specific arrangement of the α-MnO_2 crystals into the rosettes seems to be achieved by fast evaporation of upwards migrating solutions from the tectonic zone. The last in this succession is calcite cement filling the pores, mainly in the upper part of the travertine frame. Generally, this was abiologically mediated process of precipitation of calcium carbonate due to rapid degassing of carbon dioxide and occasionally, in the top of the travertine dome, due to direct precipitation from the ground waters.

Key words: Precipitation of calcium carbonate, Manganese oxides, Travertine, Holocene, Tectonic dislocations, Holy Cross Mts.

INTRODUCTION

According to SANDERS & FRIEDMAN (1967) travertine can be understood as all non-marine limestone accumulations formed in lakes, rivers, springs and caves. However, within all other English speaking cultures those calcareous deposits have been called tufas (FORD & PEDLEY 1996), which is similar in Polish terminology, apart from speleothems i.e. cave limestone accumulations (SZULC 1983). There are still different points of view on all those deposits describing finely crystalline deposit or incrustation formed by rapid precipitation of calcium carbonate from cold or thermal waters in a surface environment as travertine (TURI

1986) or even adopting the term travertine for all above mentioned deposits (PENTECOST 1993, 1995; PENTECOST & VILLES 1994). We have followed FORD & PEDLEY (1996) terminology. For the purpose of the present paper we use the term travertine as a synonym of thermal or hydrothermal calcareous deposits which lack visible organic remains, whereas tufa maens to us all the calcareous deposits derived from land waters of cool and ambient temperature. Therefore, calcareous deposits observed in Carpathian Mountains (HALICKI & LILPOP 1932, GRUSZCZYŃSKI & MASTELLA 1986, ČABALOVA 1991, MASTELLA 2001, ALEXANDROWICZ & GERLACH 1983) should be called tufas, for they form incrustations on plants or vegetal remains due to rapid precipitation of calcium carbonate from hydrothermal and/or surface waters. The hydrothermal origin of those tufas is not so apparent as in the case of the young, active tectonic regions such as Aegean or northern Apennines, or Basin and Range Province in the USA where calcareous deposits – travertines, in this

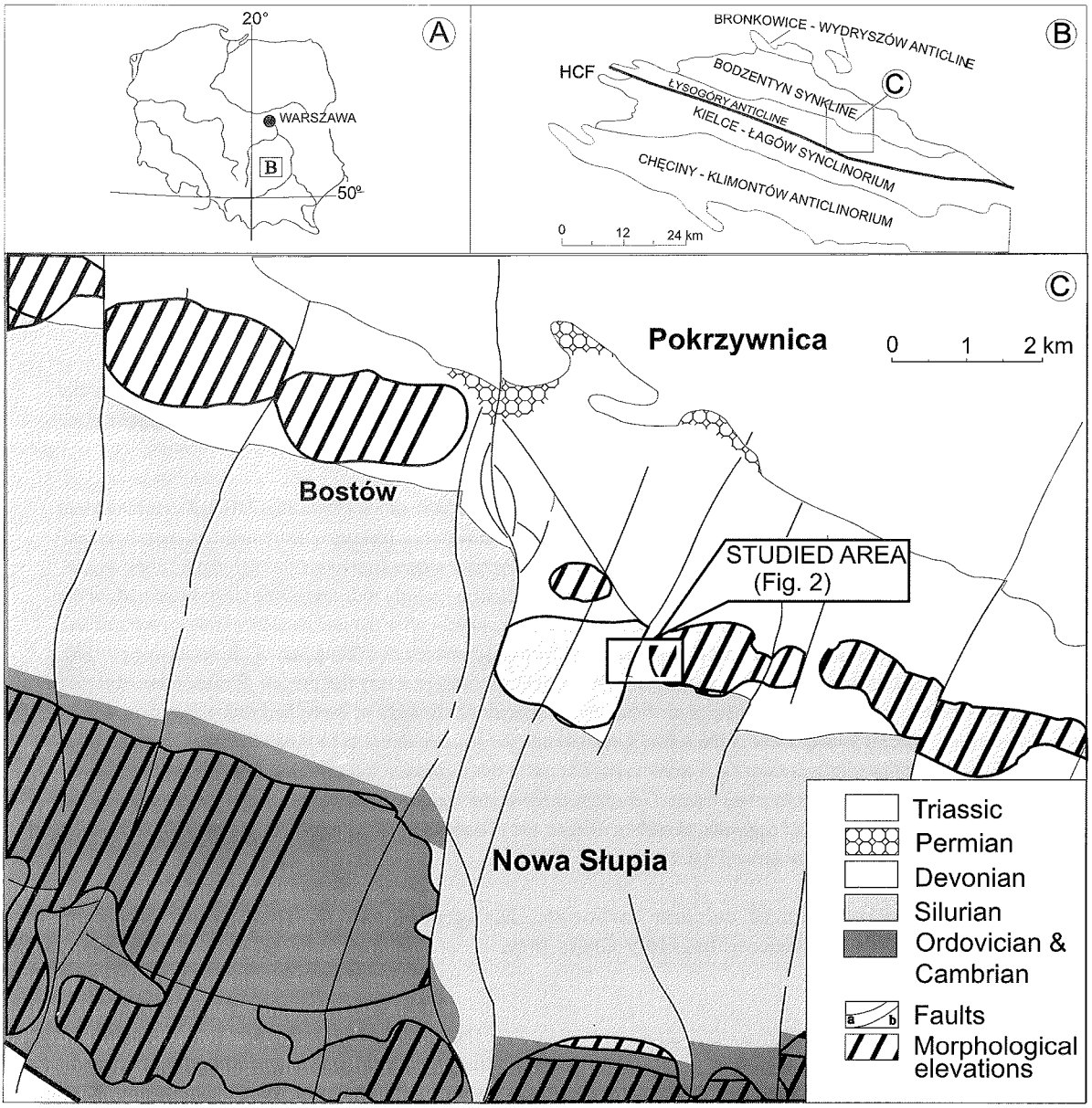

Fig. 1. A – Sketch-map of Poland with location of the Holy Cross Mountains marked by a rectangle; B – The major structural units of the Holy Cross Mountains (HCF = Holy Cross Fault) with location of the general area with travertine occurrences; C – Geological sketch-map of the general area with travertine occurrences and with location of the studied area presented in Text-fig. 2

case, form gigantic positive morphological structures within the fault zones (HANCOCK & *al.* 1999). The phenomenon such as a large calcareous dome discovered (CZARNOCKI 1928; FILONOWICZ 1968, 1969, 1980) within the old Palaeozoic tectonic region (Text-fig. 1), of the Holy Cross Mts., Central Poland, is rather unique. FILONOWICZ (1968, 1969) considered the calcareous dome of the Holy Cross Mts. to be created rather by carbonate rich rain and occasionall snow melt waters percolating through loess covers adjacent to the travertine (Text-fig. 2), rather than by hydrothermal water reaching the surface through the fissures within the fault zone (Text-fig. 2). Therefore, the main purpose of the present paper was, after defining the age of the calcareous dome, to look through the main petrographic and geochemical features of the internal structure of the dome in an attempt to solve the problem of its origin. Secondly we wanted to look in details at the carbonate and other minerals crystal forms of the internal structure expecting some specific appearances.

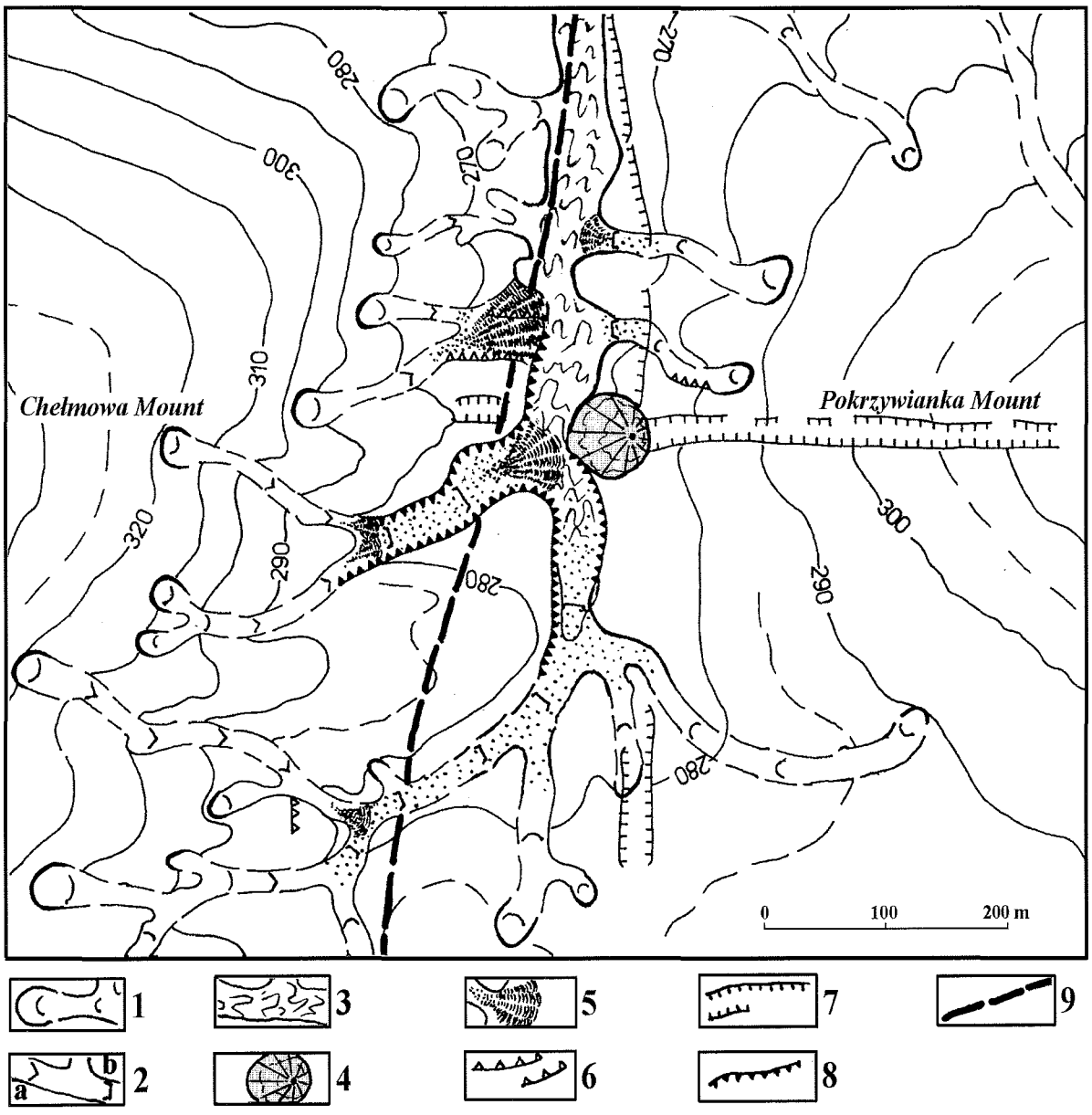

Fig. 2. Geomorphological sketch (of the area marked in Fig. 1) showing location of the calcareous dome against the main fault and the system of little valleys of different origin developed within the fault zone. 1) trough valley; 2a) gills; 2b) gorges; 3} troughs; 4) calcareous deposit dome; 5) alluvial fans of silts; 6) agriculture terraces; 7) road cuts; 8) erosional cuts; 9) faults

Geological position of the calcareous dome

Despite controversies about whether there were two diastrophic events (Caledonian and Variscian according to DADLEZ & *al.* 1994, ZNOSKO 1995, KOWALCZEWSKI & DADLEZ 1996), or only one, Variscian orogenetic event (MIZERSKI 1995, 2000) in the Łysogóry Unit, there were two domains formed (Łysogóry Anticline and Bodzentyn Syncline). The whole Łysogóry Unit defined mainly by transverse faults, steep normal and translation faults. The major component of this tectonic system is the Łysogóry Fault (CZARNOCKI 1950, MIZERSKI 1978) with a group of minor faults attached to the major fault (Text-fig. 1). Considerable new evidence of neotectonic and contemporaneous tectonic activity has been recently observed in the zone of the Łysogóry Fault (KOWALSKI 1998, 2000; MASTELLA & MIZERSKI 2002). The most visible expression of this activity is registered by nearby earthquakes (JANCZEWSKI 1932) and structural elevations and depressions (KOWALSKI 2002) causing deformations of the original river courses (middle Słupianka and middle Pokrzywianka). The examined dome lies just within the zone of secondary faulting adjacent to the Łysogóry Fault (Text-figs 1, 2). It is a normal-translation fault of NNE-SSW direction cutting through Devonian siliciclastic sedimentary sequences of clays, silts and sandstones.

General description of the calcareous deposit

The examined calcareous deposit is extremely hard rock without any visible organic remains within the rock. Assuming its location within the zone of faulting and the observed structure we called travertine the examined deposit. The travertine is located in the depression of the passage between Chełmowa Hill and Pokrzywianka Hill (Text-fig. 2), and represents a geological tourist attraction (STUPNICKA & STEMPIEŃ-SAŁEK 2001). The travertine forms an almost circular dome morphologically of, at least, 7 m height and 60 m in diameter (Text-fig. 2). The dome is quite asymmetrical for it was cut during the road work. The slopes of the dome are quite gentle (from 8-14 degrees).

MATERIAL AND METHODS

We have taken several tens of samples from the top of the travertine dome and from the bottom about a meter above the contact between the travertine and Devonian sandstones of the Palaeozoic basement. All the samples were carefully washed to remove contamination. Some of the samples were treated with acetic acid to establish the presence of any structures resembling crystal or bacterial shrubs (CHAFETZ & FOLK 1984, CHAFETZ & GUIDRY 1999) flat-cut surfaces and sent for age determination. Some other samples were thin sectioned and these, polished thin sections were used for petrographic investigations under polarized microscopy. After carbon coating, selected thin sections were examined using the SEM Philips XL-40 for detailed distribution and appearance of major mineral components of the travertine due to BSE and EDAX examinations. Chips of the fractured rock samples, some of them etched in 0.5% acetic acid, were examined using SEM and BSE images to identify the distribution and texture of the mineral constituents of the travertine. We have selected samples for stable carbon and oxygen isotope ratios analyses; three pieces among the several tens of samples from the top and three pieces among the ten samples from the bottom of the travertine. All these pieces were randomly chosen. Powdered calcium carbonate of the selected pieces were analysed for the $^{13}C/^{12}C$ and $^{18}O/^{16}O$ ratios using Finigan MAT DELTA+ mass spectrometer, housed at the common laboratory of the Institute of Paleobiology and Institute of Geological Sciences Polish Academy of Sciences, and the results have been calculated versus PDB.

AGE DETERMINATIONS AND SEM OBSERVATIONS, AND GEOCHEMISTRY OF THE TRAVERTINE

The major component of the travertine either at the top or in the bottom of the dome is micritic calcite (FOLK 1965, BATHURST 1971). And this micrite seems to be the primary deposit in the travertine frame. Within the micrite there have been found randomly distributed quartz grains,

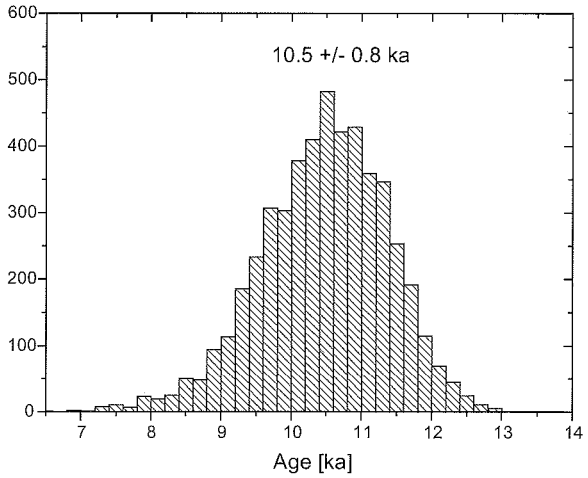

Fig. 3. Age distribution for basal layer of the calcareous dome obtained using randomisation method

sometimes distributed into patches or layers. There is also some kaolinite in the upper part of the travertine. In the bottom part of the travertine, quartz grains are usully stained with manganese oxides. There are also rare grains of TiO_2 – rutile or anatas and most presumably loess granules visible as aggregates of minute quartz grains.

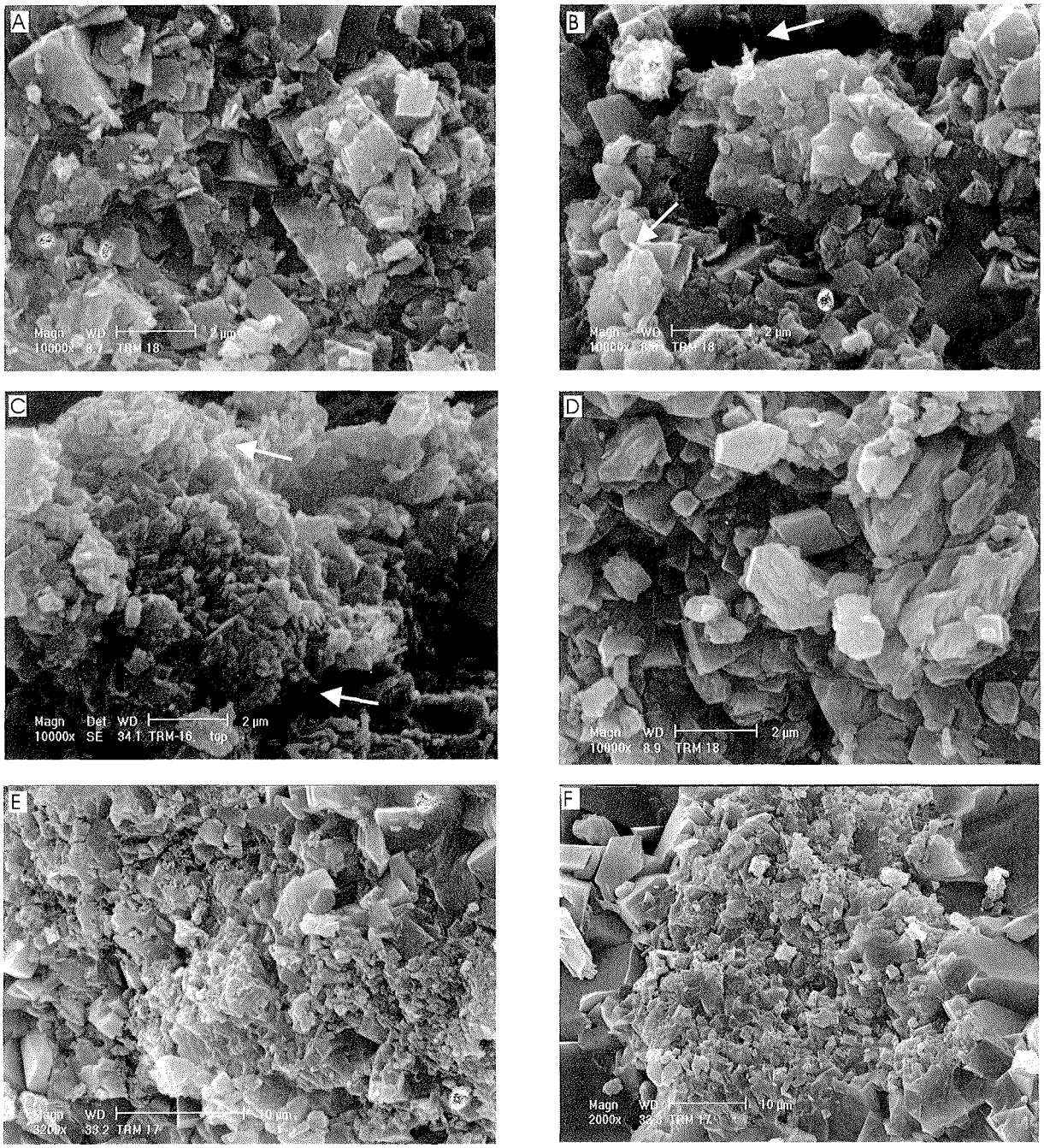

Fig. 4. A – SEM image of the calcite rhombs and other composite scalenohedral crystals in the upper part of the travertine. Some of the crystals are of skeletal appearance and the others display dendritic outer shape. B – SEM image of the abundant composite calcite crystals with minute crystallites protruding out of the crystals (arrows). These crystallites are probably calcified rods of bacilliform bacteria. Note the shield-like calcite crystals in some places covering another crystal. C – SEM image of a bundle of minute rod and rod tips and calcified bacilliform bacteria rods protruding out of the crystal mass (arrows). D – SEM image of the minute calcite rhombs mixed with larger composite crystals. E and F are SEM images of the remains of the micrite matrix in the bottom part of the travertine. E – SEM image showing an aggregate of rounded nannometre-scale crystallites at the surface of the larger calcite blocky crystals. F – SEM image of individualised patch of an aggregate of nannometre-scale crystallites surrounded by pure blocky calcite crystals

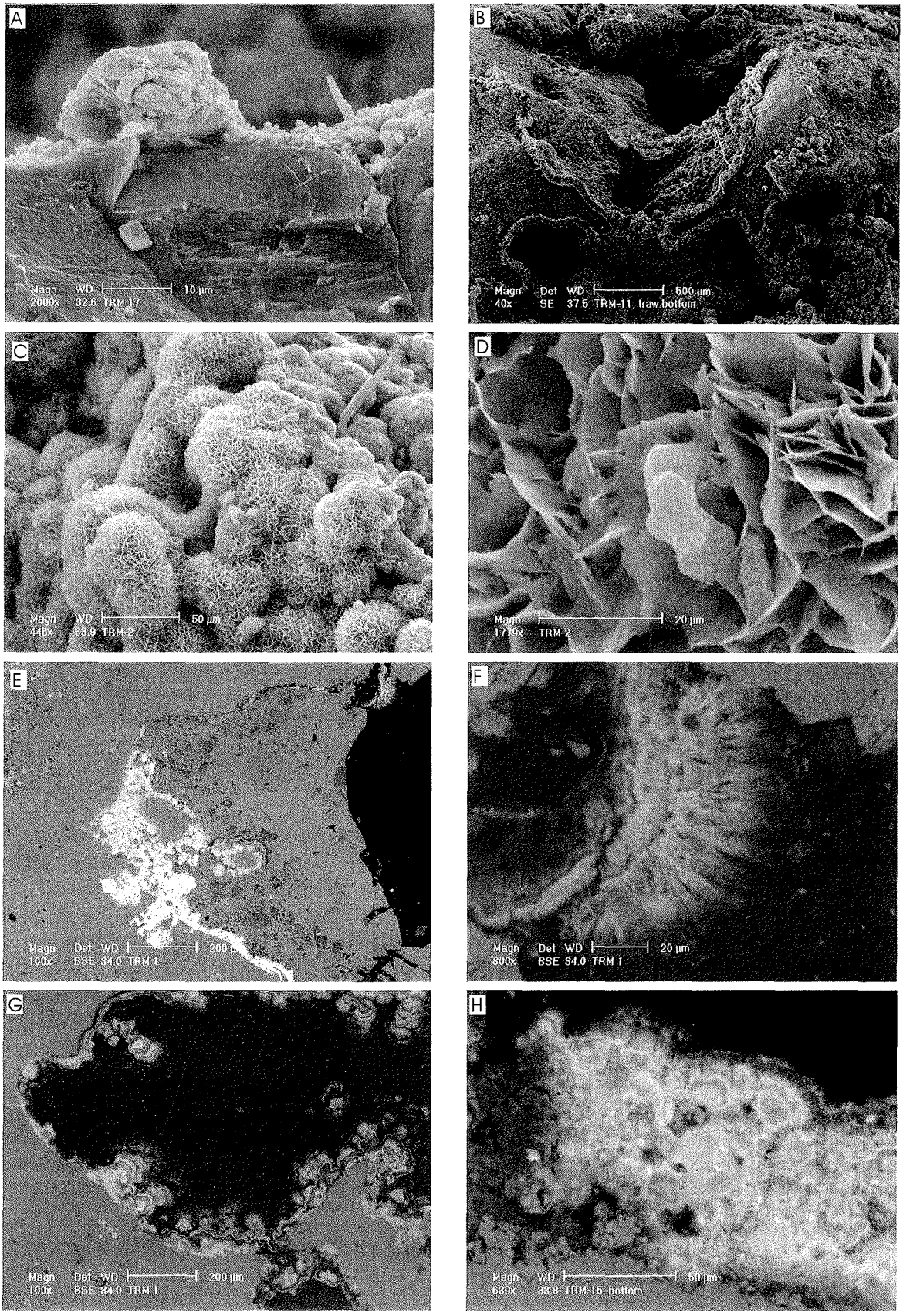
A
Magn WD 10 µm
2000x 32.6 TRM-17
B
Magn Det WD 500 µm
40x SE 37.5 TRM-11, traw bottom
C
Magn WD 50 µm
445x 33.9 TRM-2
D
Magn 20 µm
1770x TRM-2
E
Magn Det WD 200 µm
100x BSE 34.0 TRM 1
F
Magn Det WD 20 µm
800x BSE 34.0 TRM 1
G
Magn Det WD 200 µm
100x BSE 34.0 TRM 1
H
Magn WD 50 µm
639x 33.8 TRM-15, bottom

The age of the travertine

Basal layers of the travertine dome has been analysed using U-series method in the U-series Laboratory of the Institute of Geological Sciences of the Polish Academy of Sciences (Warsaw, Poland). It was necessary to a perform correction for the detrital contamination by non-radiogenic U and Th isotopes using isochrones method. Classical LL method has been used (PRZYBYŁOWICZ & *al.* 1991). The sample has been divided in 6 sub-samples with different calcite – detritus proportions. Each of the sub-samples has been analysed using standard chemical procedure of Uranium and Thorium separation from carbonates (IVANOVICH & HARMON 1992). The samples were dissolved in 6 M nitric acid, and uranium and thorium were separated by a chromatographic method using the DOWEX 1x8 ion exchanger. The efficiency of chemical separation was controlled by addition of a ^{228}Th - ^{232}U spike. Activity measurements (α spectrometry) were obtained on a OCTETE PC spectromether of the EG&G ORTEC company. Spectrum analysis and activity calculation were performed with the use of "URANOTHOR 2.5" software (GÓRKA 2002). Isochrones construction and corrected activity ratios have been calculated using Randomisation method (monte carlo type procedure) (HERCMAN & DEBAENE 2003).

Corrected actrivity ratios used for age calculations are: $^{234}U/^{238}U = 2.42 \pm 0.07$, $^{230}Th/^{234}U = 0.092 \pm 0.008$. Isochrone age of the sample is: 10.5 +/– 0.8 ka and the age distribution is presented in the Text-fig. 3.

SEM observations

Primary deposit

Micrite matrix in the upper part of the travertine displays a wide range of arrangement of calcite crystals. There are parts of rhombic and other scalenohedral composite crystals (Text-fig. 4A). Some of those crystals are of skeletal appearance, and in other maintain remains of the individual crystallites. Individual calcite rhombs are usually 700-800 nm in diameter. There are other parts, where larger composite crystals are composed of amoeba-like crystallites and minute rhombs (Text-fig. 4B), or an aggregate of rounded nanometre-scale crystallites (Text-fig. 4C). Interestingly some crystallites protrude out of the crystals and appear to be calcified rods of bacilliform bacteria (Text-fig. 4B-C). Some of the rods as well as nanometre-scale rounded crystallites are visible to be merged in the crystal faces (Text-fig. 4B-C). There are also parts in the micrite matrix which show fewer composite crystals, or rhombs and do not show individual crystallites within them (Text-fig. 4D).

This intensive recrystallization must have occurred in the bottom part of the travertine for we can find only remains of the micrite matrix (Text-fig. 4E-F). The most common type of the structure is an aggregate of rounded nanometre-scale crystallites at the surface of the larger calcite blocky crystals (Text-fig. 4E). One can also find an individualised patches of an aggregate of nanometre-scale crystallites surrounded by pure blocky calcite crystals (Text-fig. 4F). Those blocky crystals are usually lining the pores in the travertine allowing precipitation of the manganese oxides and occasionally bizzare composite calcite crystals (resembling gothic-like crystals, FOLK & *al.* 1985) inside a pore among the manganese precipitate (Text-fig. 5A).

Secondary deposit

The manganese is rather unique. According to the microchemical analyses it is a pure α-MnO_2. Unlike other manganese oxide forming mixed species enriched in Ba, K, and Pb (BOLEWSKI 1965), the examined α-MnO_2 shows only about 4% of BaO, compare to the most common in nature psylomelane of at least 10% of BaO plus other alkali metal oxides admixtures (BOLEWSKI 1965), and more interestingly 2% of HgO. The α-MnO_2 precipitate is the main component occuring in the pores of the bottom part of the travertine frame (Text-fig. 5B). It also fills fissures and cracks in the micrite matrix mainly in the bottom part of the travertine (Text-fig. 5E). In the case of the bottom part of the

Fig. 5. A – SEM image of the composite calcite crystal (resembling gothic-like crystals – FOLK & *al.* 1985) surviving inside a pore among the α-MnO_2 precipitate. B – SEM image of the α-MnO_2 lining and filling the pores within the travertine frame. Slightly etched, with acetic acid, the fractured surface of the piece of the travertine. C – SEM image of the α-MnO_2 rosettes with a fungal thread (in the upper right corner of the photograph). D – SEM image of the α-MnO_2 monoclinic crystals arranged in the rosettes. E – BSE image of the α-MnO_2 (bright colour) filling fissures and smaller pores within the travertine frame and a specific arrangement of the α-MnO_2 precipitate within the large pore of the travertine (in the upper right corner of the photograph). F – BSE image of the α-MnO_2 (brighter colour) arrangement within the large pore of the travertine showing the first generation of crystals forming rosettes followed by the second generation of acicular crystals. G – BSE image of the α-MnO_2 (bright colour) forming mushroom-like layered precipitates lining the large pore of the travertine. H – BSE image of the specific α-MnO_2 (bright colour) arrangement showing superimposed units resembling malachite structure. Interestingly, the outer rim of the α-MnO_2 units closest to the open pore display acicular arrangement of crystals

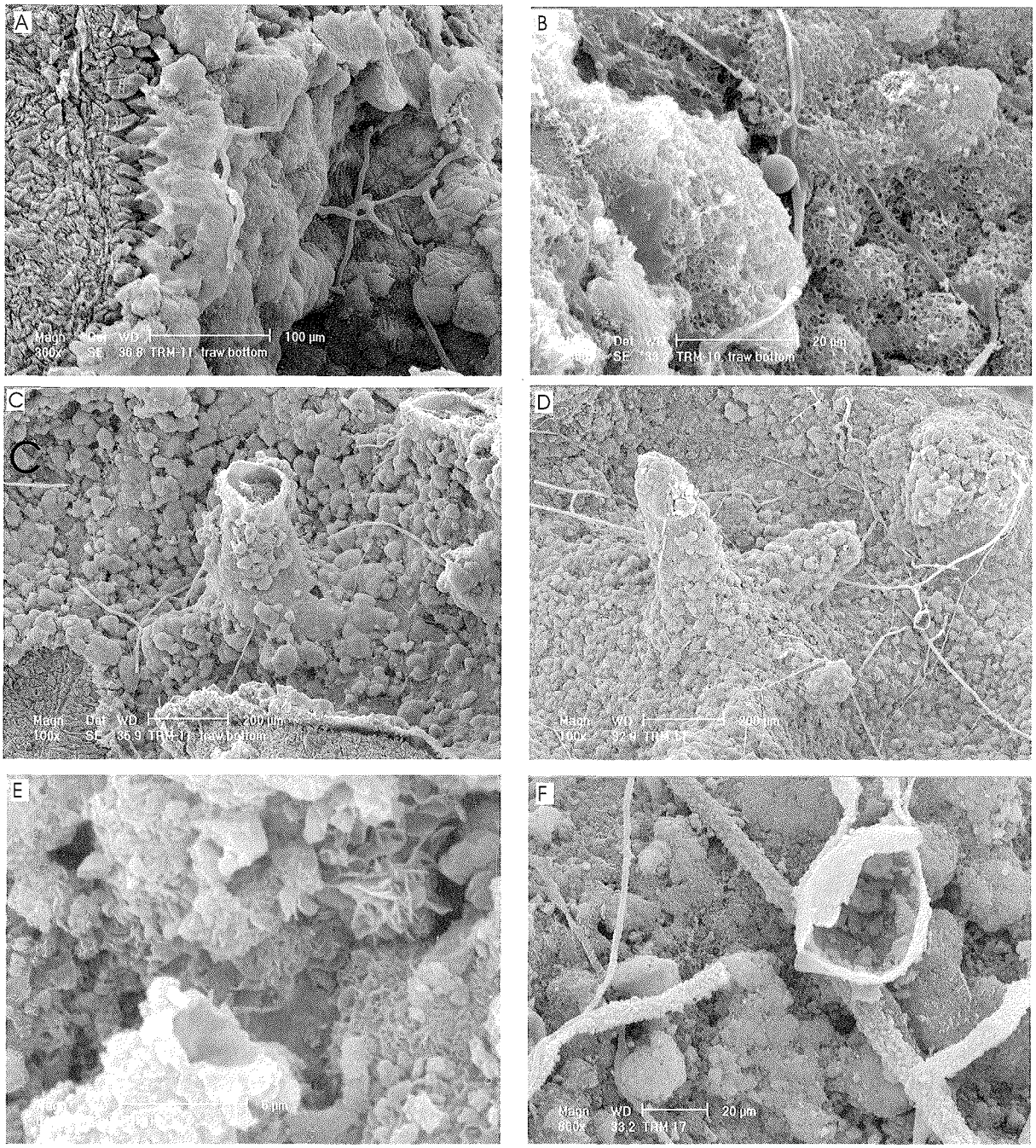

Fig. 6. A – SEM image of slightly etched, with acetic acid, surface of the fractured piece of the travertine from the bottom part of the dome, showing a pore lined with α-MnO_2 precipitates. Interestingly, precipitation of α-MnO_2 is post-dated by silicified fungal threads, therefore preserving their original shape. B – SEM image of the squashed fungal threads post-dating precipitation of α-MnO_2 rosettes. One can see a spore attached to a fungal thread (in the middle of the photograph). C – SEM image of the unidentified microbial remain (possibly cyanobacterial filament) forming, sort of, a chimney covered by α-MnO_2 rosettes and surrounded by fungal threads. D – SEM image of the unidentified microbial remains (plausible cyanobacterial filaments) forming pinnacles covered by α-MnO_2 rosettes and surrounded by abundant fungal threads with remains of the fungal spore. E – SEM image of the end fragment of the fungal tube encrusted by the α-MnO_2 precipitates. Interestingly, this encrusting cover of the fungal remains consist of irregular grains of manganese oxide rather than monoclinic crystals of α-MnO_2 precipitate forming rosettes. F – SEM image of the fungal network, some of the fungal threads squashed, and remains of the spore delicately encrusted by manganese oxide grains

travertine frame, α-MnO_2 fills smaller pores in the frame almost completely, and lines and has grown into the interior of the large pores (Text-fig. 5B). The α-MnO_2 itself is usually arranged in rosettes resembling rosettes of clay minerals such as chlorite or glauconite. The individual crystals of α-MnO_2 arranged in the rosettes are monoclinic (Text-fig. 5D) the first of two crystallographic systems reserved by BOLEWSKI (1965) for the α-MnO_2 crystals. α-MnO_2 precipitate can be of an arrangement within the large pores of the travertine frame showing the first generation of crystals forming rosettes followed by the second generation of acicular crystals (Text-fig. 5F). This is also a case of α-MnO_2 common botryoidal growth forms lining the pores of the travertine (Text-fig. 5G), where the last generation of α-MnO_2 crystals extending into the pores are of acicular arrangement (Text-fig. 5H). Siginificantly, the α-MnO_2 precipitates are associated with abundant fungal remains (Text-fig. 6). Some of the fungal threads are silicified and look fresh and intact (Text-fig. 6A), and some threads are squashed although the spores seems to be intact too (Text-fig. 6B). This microbial, i.e. fungal invasion seems to post-date the α-MnO_2 precipitates. There have also been found other, unidentified microbial remains (plausible cyanobacterial filaments resembling *Phormidium incrustatum* – JANSSEN & *al.* 1999) forming chimneys (Text-fig. 6C) or pinnacles (Text-fig. 6D) covered by a-MnO_2 rosettes and surrounded by fungal threads. The manganese oxides encrusting the fungal remain are rather irregular grains, and not the monoclinic crystals of the α-MnO_2 forming rosettes (Text-fig. 6E). The fungal network display some individuals which are squashed too, and remains of the spore however full of manganese is only slightly encrusted by the manganese oxide grains (Text-fig. 8F).

Later cements

In the upper part of the travertine dome the pores are filled with a dense mass of bizarre looking calcite crystals (Text-fig. 7). These crystals show a skeletal character with many fibre-like or spiky crystallites visible on the crystal faces of elongated crystals with poorly developed terminations and crystals with cavities in terminal faces (Text-fig. 7A). Close up views on a few crystals show details of the spiky features and undeveloped terminations of the elongated crystals. The holes appear to be empty spaces caused by the absence of single or bundles of crystallites developed terminal faces (Text-fig. 7B). A close up view on of the other cement crystals shows their skeletal appearance (Text-fig. 7C). An example of the spiky features of single calcite crystal without crystal faces but showing two different directions of the calcite fibers is seen in (Text-fig. 7D). There are other types of the crystal assemblages filling the pores in the upper part of the travertine frame. These are composed of fully developed, densely packed scalenohedra. Some of the crystals display specific ornament (little spikes) on the crystal faces (Text-fig. 7E). Exactly the same single crystals fill occasionally the circular pores, 30-40μm in diameter, occurring an association within the micrite frame (Text-fig. 7F). There are also nests of lublinite-like crystals (Text-fig. 7G). Lublinite, distinguished by MOROZEWICZ (1907) as distinct calcite species because of being calcite rhombohedrons extremely elongated along (1011): (1101) edge, was found in the „moon milk" precipitates in the caves (GRADZIŃSKI & RADOMSKI 1957, ASSERETO & FOLK 1980). And close observation of calcite specimens from the original MOROZEWICZ's locality (GRUSZCZYŃSKI in prep.) have presented lublinite as a n assemblage of variable, rarely single what MOROZEWICZ (1907) thought, more often composite crystals, some time much more complex than *en echelon* stacking of the crystals to form a needle (STOOPS 1976). In our case, the dense mat of lublinite-like calcite crystals is not very thick, it is just a lining of the bottom of the pore within the travertine frame (Text-fig. 7G). Close up view on the single needles within the mat reveal composite structure of some needles (Text-fig. 7H).

The later cement in the pores within the bottom part of the travertine frame is represented by the mass of bizarre calcite crystals (Text-fig. 8A). SEM image of the enlarged bizarre crystals reveal spheres, some composite but many rounded and rod-like crystallite forms (Text-fig. 8B). Within the calcite composite crystals filling the pore we have found unexpectedly unidentified microbial, silicified bulbous remains (Text-fig. 8C). The detailed SEM image of one of the unidentified microbial bulbous remain show, sort of, "crystalline byssus" binding microbial "cyst" to the mass of crystals (Text-fig. 8D).

Stable isotope geochemistry of the travertine calcium carbonate

All the samples examined, either from the top or the bottom of the travertine dome have shown the $\delta^{13}C$ and $\delta^{18}O$ values in the very narrow range of 0.2 and 0.4‰ respectively. The mean value of the $\delta^{13}C$ for the upper part of the travertine is –10.7‰ PDB, whereas that value for the bottom part of the travertine is –10.1‰ PDB. In the case of the $\delta^{18}O$ mean values the difference between the upper and bottom part of the travertine is almost negligible, which means the $\delta^{18}O$ mean value for the upper part of the travertine is –8.1‰ and for the lower part that value is –7.9‰.

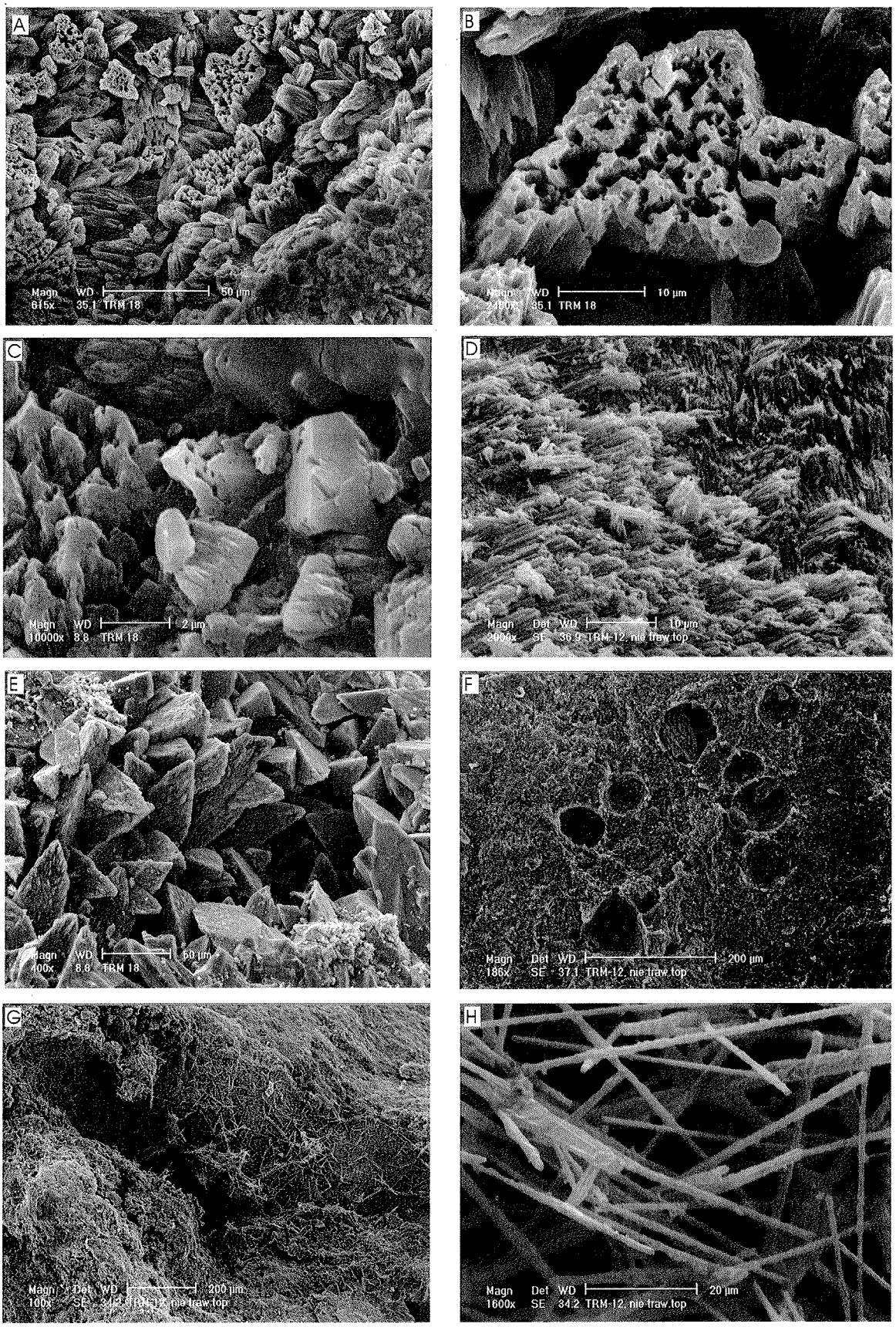
A
Magn WD 50 µm
615x 35.1 TRM 18
B
Magn WD 10 µm
2400x 35.1 TRM 18
C
Magn WD 2 µm
10000x 8.8 TRM 18
D
Magn Det WD 10 µm
2000x SE 36.9 TRM-12_nie traw.top
E
Magn WD 50 µm
400x 8.6 TRM 18
F
Magn Det WD 200 µm
186x SE 37.1 TRM-12_nie traw.top
G
Magn Det WD 200 µm
100x SE 34.2 TRM-12_nie traw.top
H
Magn Det WD 20 µm
1600x SE 34.2 TRM-12_nie traw.top

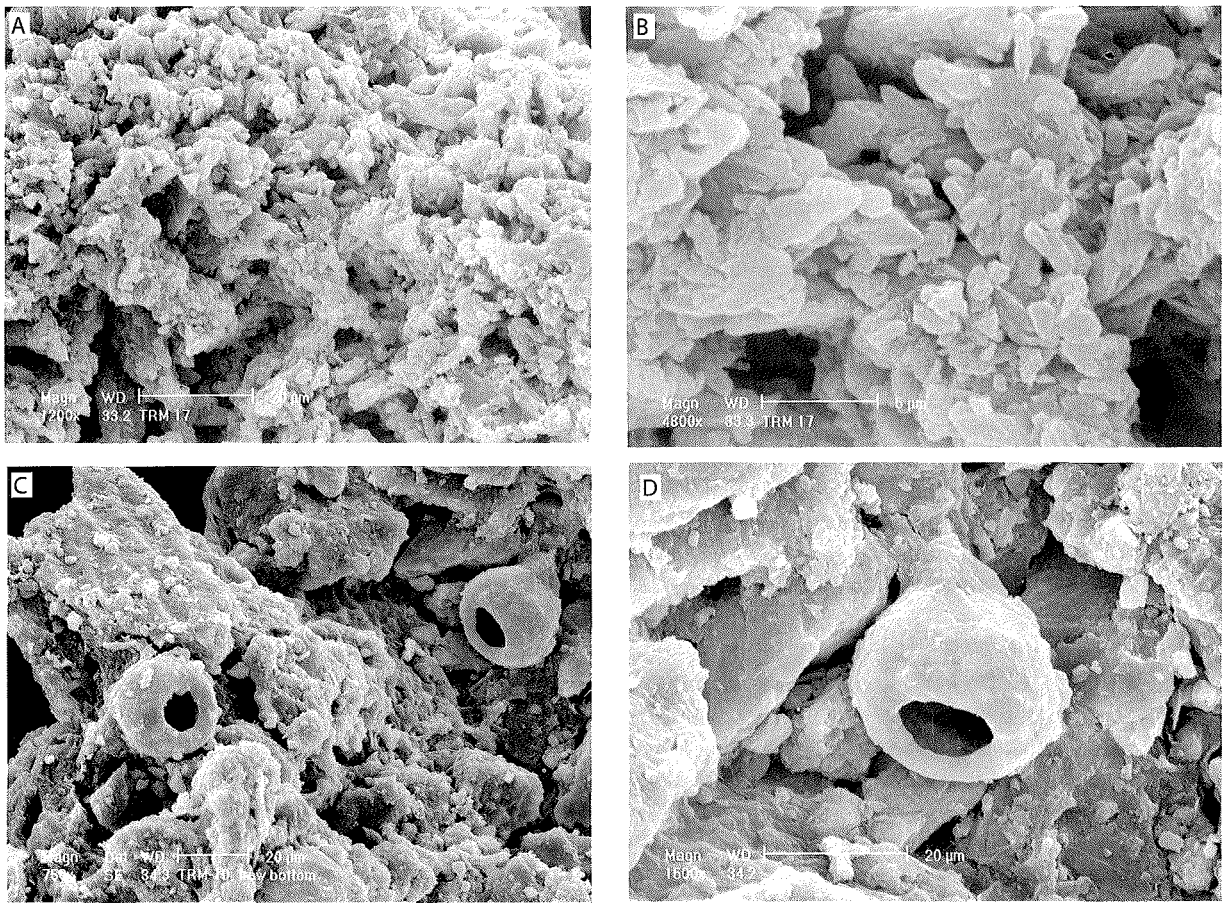

Fig. 8. A. SEM image of the mess of bizarre calcite crystals filling one of the pores within the travertine frame from the bottom part of the dome. B. SEM image of the enlarged bizarre crystals, some rounded arranged in, sort of, circles, some composite of skeletal amoebas appearance with many rounded and rod-like crystallites merged in the crystals. C. SEM image of the unidentified microbial, silicified bulbous remains (possibly fungal spore cases) within the calcite composite crystals filling one among the pores of bottom part of the travertine frame. D. SEM image of one of the unidentified microbial bulbous remain showing the details of its structure

ORIGIN OF THE CALCITE AND α-MnO_2 PRECIPITATES

There is no doubt, all the crystallite rods stretching out of the crystals or merged in the crystal faces observed within the travertine micrite are calcified bacilliform bacteria rods. The rods are identical with those described in many papers devoted to bacterial carbonates (CHAFETZ & FOLK 1984; FOLK 1993, 1999; LOISY & *al.* 1999). There are also similarities of single composite rhombs to the gothic-like crystals described by FOLK & *al.* (1985) as well as shield-like crystal envelopes to the degraded crystals also described by FOLK & *al.* (1985). Also, a dense mess of nanometre-scale crystallites is very similar to bacterial

Fig. 7. A – SEM image of densely packed calcite crystals within the pore of the travertine frame from the upper part of the dome, showing partly developed crystals with holes in terminal crystal faces and spike features on the other crystal faces. B – SEM image of a few crystals visible in A, showing details of the spiky features and the cavities. C – SEM image of the several undeveloped crystals of skeletal appearance showing very clear spiky features. D – SEM image of the classical example of the spiky features of the single calcite crystal without two crystal faces developed, filling the pore in the upper part of the travertine frame. The different directions of the calcite fibers related to two undeveloped crystal faces. E – SEM image of densely packed scalenohedral crystals filling totally a small pore of the travertine from the upper part of the dome. Note, the specific ornament (spikes) on some crystal faces (the left part of the photograph). F – SEM image of the association of circular pores of 30-40μm in diameter filled occasionally with single scalenohedral calcite crystals with specific ornament on the crystal face (spikes). G – SEM image of the dense mat of lublinite-like calcite crystals. H – SEM image of the fragment of the mat of the calcite precipitate showing lublinite-like crystals. Some of those crystals seems to be composite

debris used in experimental calcite precipitation (KIRKLAND & *al.* 1999). Of course, it is a matter of dispute about nanometre-scale rounded objects, batons and balls (FOLK & LYNCH 2001) so abundant in the travertine could have been bacteria or not. According to experiments (KIRKLAND & *al.* 1999) nanometre-scale proto-crystals and crystals can easily be produced from the solution highly supersaturated with respect to calcium carbonate with and without high content of dissolved organic carbon content. This suggestion might be relevant in the case of minute (600-800 nm in diameter) anhedral calcite rhombic and scalenohedra crystals from the travertine. It is also a matter of dispute whether bacteria which have been calcified were sulphur-oxidizing bacteria as those involved in formation of world known Italian travertines (CHAFETZ & FOLK 1984; FOLK & *al.* 1985) or other kind of bacteria involved in the process of calcification (KRUMBEIN 1979, CASTANIER & *al.* 1999). However, sulphur-oxidizing bacteria precipitate calcium carbonate and also elemental sulphur (CHAFETZ & FOLK 1984). There is some, up to 2% wt, of sulphur detected within the micrite frame, and crystals resembling gothic-like or carapace crystals being originated in the environment of sulphur-oxidizing bacteria (FOLK & *al.* 1985). However this may be insufficient to classify bacteria observed within the examined travertine.

Nevertheless, we suggest a part, at least, of the calcite travertine frame crystallized on bacterial precursor. As for the conditions favourable for precipitation of the travertine calcite we may suggest the solution highly supersaturated with respect to calcium carbonate (see for comparison PEDLEY 2000). Apart form many rhombic and amoeboidal crystals similar to those formed under conditions of high supersaturation with respect to calcium carbonate (CHAFETZ & *al.* 1991, KIRKLAND & *al.* 1999), may have been circular pores of 60 to 80 μm in diameter within the travertine frame which supposedly were gas bubbles of carbon dioxide or hydrogen sulphide? trapped while spontaneous precipitation of calcite occurred. The bubbles are substantially smaller than those described by CHAFETZ & *al.* (1991), however the conditions of uneven high supersaturation with respect to calcite might be similar. In the case of the travertine calcite, supesaturation must have been achieved by rapid degassing of CO_2.

Additional information on the origin of the travertine frame may be obtained by considering precipitation of the α-MnO_2 succeeding calcite micrite. Source of manganese in a divalent state to be later oxidized can be natural (STUMM & MORGAN 1970) or volcanic (ICHIKUNI 1973) waters. High solubility of Mn^{2+} is kept at low Eh and pH conditions (HEM 1963), and high specific organic matter content i.e. tannins and anaerobic degradation of plant detritus keep manganese in the Mn^{2+} state (HEM 1964). Increase in pH and high bicarbonate activity provide precipitation of calcium carbonate with high content of manganese, whereas increase in Eh caused rapid oxidation of Mn and formation of manganese oxides. However, such a scenario has never been observed in natural waters and soils (MOUNT & COHEN 1984). There is a high content of Mn in calcite under low Eh, high pH and high organic matter content conditions, and low content of Mn in calcite under low organic content and high Eh, pH conditions. However there is low manganese oxides in the latter case (MOUNT & COHEN 1984). Therefore, the α-MnO_2 in the examined travertine cannot be precipitated due to processes occurring in the ground waters and soils. Assuming source of Mn^{2+} is endogenic (hydrothermal), there should have been a rapid change in Eh causing rapid oxidation of manganese and its precipitation. The α-MnO_2 crystals arrangement in the rosettes resembles the arrangement of gypsum crystals in the "desert roses" and leads to a conclusion of fast evaporation of the manganese bearing solution. Some of the Mn^{2+} seems to be oxidize by fungi, for it has been well known that certain groups of fungi such as *Cephalosporia* and *Cladosporia* act this way (MARSHALL 1979, see also ERLICH 1996). In this case, manganese oxide precipitate on some fungal remains might be the result of activity of the bacterium *Metallogenium symbionticum* possessing filaments surrounded by MnO_2 (ZAVARZIN 1961, 1963). The fungal remains covered by manganese oxide flakes, postdating α-MnO_2 precipitate by hydrothermal solution, clearly indicate that the Mn later precipitates are ongoing and very modern (PEDLEY 2003, *pers. inf.*) and may not have been connected with hydrothermal solutions.

The later calcite cement filling the pores within the upper part of the travertine frame are of two types. The first is composed of crystals of spiky appearance, not fully developed very similar to those formed in the hot springs (FOLK & *al.* 1985) or waters highly supersaturated with respect to calcium carbonate (CHAFETZ & *al.* 1991). Therefore we suggest abiological, rapid precipitation of calcium carbonate rapid enough to form skeletal crystals, rather than crystallization of calcite on any microbiological precursor. Precipitation seems to have occurred from a solution which might have been a mixture of hydrothermal and ground waters causing rapid degassing of carbon dioxide. This in turn led to spontaneous precipitation of calcium carbonate. The other type of calcite cement consisting of fully developed crystals typical for natural land waters precipitation (CHAFETZ & *al.* 1985, CHAFETZ & GUIDRY 1999) appears not to be influenced by hydrothermal waters. The origin of specific lublinite-like crystals, which is very common precipitate as a late stage cement in tufas (PEDLEY 2003, *pers. inf.*), is a matter of dispute. FOLK & *al.* (1985) felt lublinite-like crystals had formed

during evaporation when the bacterial-mat pond had dried out. This may be the case of the lublinite-like precipitate in the top of the travertine, however some of the lublinite-like needles might also have developed on the threadlike and bacilliform bacteria nuclei. It has been well known that calcified threadlike and bacilliform bacteria rods crystalise exactly as lublinite crystals and show the same faces as lublinite-like rods (LOISY & *al.* 1999). Nevertheless, the lublinite-like cements hardly could originate from hydrothermal solutions. The calcite fill of the pores within the bottom part of the travertine is difficult to explain as a abiologically mediated precipitate of calcium carbonate because we observe nannometre-scale objects (batons, balls, rods) suggesting a microbial precursor. However, we have not observed evident bacteria rods or other microbial remains, apart from two unidentified cysts resembling common in tufas fungal spore cases (PEDLEY 2003, *pers. inf.*).

Interpretation of stable isotope geochemistry results is rather complex. In the $\delta^{13}C$ values we cannot observed any gradient changing systematically as we observed in continuously increasing the $\delta^{13}C$ values in recently formed travertines and tufas (CHAFETZ & *al.* 1991; CHAFETZ & *al.* 1991, CHAFETZ & LAWRENCE 1994). There is a little difference in the range of 1‰ pointing out in the bottom part of the travertine displaying higher values, just less than –10‰, and the upper part of the travertine displaying lower values, close to –11‰. However, this might be an effect of recrystallization of the calcite micrite in the bottom part. Older travertines (CHAFETZ & *al.* 1991) as well as diagenetically more subdued parts of the tufas usually show higher $\delta^{13}C$ values than their younger or more intact counterparts (JANSSEN & *al.* 1999). Generally, the $\delta^{13}C$ values less than – 10‰ are beyond the values typical for the travertines (TURI 1986), apart from unusual travertines from California (O'NEIL & BARNES 1971). Environmentally, the $\delta^{13}C$ of –10 to –11‰ are typical for calcium carbonate precipitating from organic rich soils or ground waters (DEINES 1980, ANDERSON & ARTHUR 1983), and marine sediments where aerobic or anaerobic oxidation of organic matter occurs (IRWIN & *al.* 1977, COLEMAN 1985). However, this seems not to be the case of the examined travertine. Assuming the hydrothermal origin of the travertine the observed $\delta^{13}C$ values are quite plausible. We do not know the exact values of the $\delta^{13}C$ for the hydrothermal waters circulating through the fault zone, for the carbon dioxide from igneous sources may reach the wide range of the $\delta^{13}C$ values (HOEFS 1997 and references therein). Mantle derived CO_2 has $\delta^{13}C$ values of –8 to –5‰, from mofettes and fumaroles –8 to –3‰, and over hot lavas –26 to –15‰. In the case of the travertine, we have to assume very high pressure of pCO_2 in the hydrothermal waters achieving very negative $\delta^{13}C$ values (see HOEFS 1997). Rapid degassing of carbon dioxide led to spontaneous precipitation of $CaCO_3$ enriched in the light isotope of carbon. It might be also an additional effect of the hydrothermal waters forming a thin film of Ca^{2+} - OH^- waters reacting with the atmospheric carbon dioxide and leading to precipitation of calcium carbonate highly enriched in the light isotope of carbon (O'NEIL & BARNES 1971). As for the $\delta^{18}O$ values these are typical of most of the travertines around the world (TURI 1986). However the first approximation, viewing travertine as a calcium carbonate precipitate formed from meteoric water does not seem appropriate. It is rather a combined effect of fast evaporation of the hydrothermal waters causing enrichment in the heavy isotope of oxygen (EPSTEIN & MAEYDA 1953) and the thin film of Ca^{2+} - OH^- waters reacting with the atmospheric carbon dioxide leading to drastic depletion in the heavy isotope of oxygen (O'NEIL & BARNES 1971).

CONCLUSIONS

All the petrological and geochemical investigation of the large calcareous dome developed in the middle of the Holy Cross Mts. (Central Poland) suggest its origin as being created by the hydrothermal rather than ground or meteoric waters. This travertine dome is of Holocene age. Therefore, Holocene tectonic activity of the main fault of the Palaeozoic substratum seems to be the reason of the hydrothermal water circulation through the fault zone. Interpretation of the stable isotope geochemistry results, although rather complex, seem to confirm the scenario of the hydrothermal waters circulation through the rejuvenated fault zone causing formation of the unusual travertine dome.

The formation of the internal structure of the examined travertine encompasses several successive stages, which are as follows:

1. A main body of the travertine was built up of micritic calcite. This was extremely rapidly crystallized calcite from highly supersaturated solution derived. Some of these calcite crystals display remains of calcified bacilliform bacteria rods suggesting an essential part, at least, of calcite was crystallized on a bacterial precursor.

2. Successively, after the micrite calcite travertine frame had been formed, almost pure (having only barium and mercury as additional components) monoclinic manganese oxide (α-MnO_2) precipitated filling part of the remaining porosity. The unique characteristics of manganese oxide crystallization also suggests a very fast process of manganese oxidation due to increase in Eh and

activity of abundant fungal species which might be associated with specific symbiotic bacterium. Specific arrangement of the α-MnO_2 crystals into the rosettes seems to be achieved by fast evaporation of migrating upwards solution from the tectonic zone.

3. The last in this succession is rapidly precipitated calcite cement filling the pores, mainly in the upper part of the travertine frame. This was, generally, abiologically mediated process of precipitation of calcium carbonate due to rapid degassing of carbon dioxide and , in the top of the travertine dome, due to evaporation. Therefore, the solution migrating from the tectonic dislocation might mix with rain waters percolating from the upper surface of the dome, and also those rain and ground waters could eventually precipitate some of those later calcite cements.

Acknowledgments

The authors thank Cyprian KULICKI for microchemical analyses and taking SEM photographs, Krzysztof MAŁKOWSKI for isotope analyses, and Marian DZIEWIŃSKI for composing of plates. Separate thanks go to Martyn PEDLEY and Rudy SWENNEN, the journal reviewers, for constructive criticism helping the authors to produce the final version of the manuscript.

REFERENCES

ALEXANDROWICZ, S.W. & GERLACH, T. 1983. Holocene travertine from Moszczenica near Bochnia. *Studia Geomorphologica Carpatho-Balcanica*, **16**, 83-97.

ANDERSON, T.F. & ARTHUR, M.A. 1983. Stable isotopes of oxygen and carbon and their application to sedimentologic and environmental problems. *In*: M.A. ARTHUR, T.F. ANDERSON, I.R. KAPLAN, J. VEIZER & L.S. LAND (*Eds*), Stable isotopes in Sedimentary Geology. *Society of Economic Paleontologists and Mineralogists Short Course*, **10**, 1-151. Tulsa.

ASSERETO, R.L.A.M. & FOLK, R.L. 1980. Diagenetic fabrics of aragonite, calcite, and dolomite in an ancient peritidal-spelean environment: Triassic Calcare Rosso, Lombardia, Italy. *Journal of Sedimentary Petrology*, **50**, 371-394.

BATHURST, R.G.C. 1971. Carbonate sediments and their diagenesis. *In*: Developments in Sedimentology, **12**, 658 pp. *Elsevier*; Amsterdam.

BOLEWSKI, A. 1965. Mineralogia szczegółowa, 796 pp. *Wydawnictwa Geologiczne*; Warszawa.

CASTANIER, S., LE METAYER-LEVREL, G. & PERTHUISOT, J-P. 1999. Ca-carbonates precipitation and limestone genesis – the microbiogeologist point of view. *Sedimentary Geology*, **126**, 9-23.

CHAFETZ, H.S. & FOLK, R.L. 1984. Travertines: Depositonal morphology and the bacterially constructed constituents. *Journal of Sedimentary Petrology*, **54**, 289-316.

CHAFETZ, H.S. & GUIDRY, S.A. 1999. Bacterial shrubs, crystal shrubs, and ray-crystal shrubs: bacterial vs. abiotic precipitation. *Sedimentary Geology*, **126**, 57-74.

CHAFETZ, H.S. & LAWRENCE, J.R. 1994. Stable isotopic variability within modern travertines. *Geographie physique et Quaternaire*, **48**, 257-273.

CHAFETZ, H.S., RUSH, P.F. & UTECH, N.M. 1991. Microenvironmental conditions on mineralogy and habit of $CaCO_3$ precipitates: An example from an active travertine system. *Sedimentology*, **38**, 107-126.

CHAFETZ, H.S., UTECH, N.M. & FITZMAURICE, S.P. 1991. Differences in the $\delta^{13}C$ and $\delta^{18}O$ signatures of seasonal laminae comprising travertine stromatolites. *Journal of Sedimtary Petrology*, **61**, 1015-1028.

CHAFETZ, H.S., WILKINSON, B.H. & LOVE, K. M. 1985. Morphology and composition of non-marine carbonate cements in near-surface settings. *In*: N. SCHNEIDERMANN & P.M. HARRIS (*Eds*), Carbonate Cements. *Special Publication Society of Economic Paleontologists and Mineralogists*, **36**, 337-347. Tulsa.

COLEMAN, M.L. 1985 Geochemistry of diagenetic non-silicate minerals: kinetic considerations. *Philosophical Transactions of Royal Society of London A*, **315**, 39-56.

CZARNOCKI, J. 1928. Spostrzeżenia w zakresie tektoniki okolic Słupi Nowej. *Posiedzenia Naukowe PIG*, **21**, 60-61.

— 1950. Geologia regionu łysogórskiego w związku z zagadnieniem złoża rud żelaza w Rudkach. *Prace Geologiczne J. Czarnockiego*, **6a**, 5-404.

ČABALOVA, D. 1991. Travertiny Slovenska.*Geologicky Pruzkum*, **1**, 4-8.

DADLEZ, R., KOWALCZEWSKI , Z. & ZNOSKO, J. 1994. Some key problems of the pre-Permian tectonics of Poland. *Geological Quarterly*, **38**, 169-188.

DEINES, P. 1980. The isotopic composition of reduced organic carbon. *In*: P. FRITZ & J.C. FONTES (*Eds*), Handbook of Environmental Isotope Geochemistry, pp. 329-406. *Elsevier*; Amsterdam.

ERLICH, H.L. 1996. Geomicrobiology, 719 pp. *Marcel Dekker, Inc*; New York.

EPSTEIN, S. & MAEYDA, T.R. 1953. Variation of ^{18}O content of waters from natural sources. *Geochimica et Cosmochimica Acta*, **4**, 213-224.

FILONOWICZ, P. 1968. Objaśnienia do Szczegółowej mapy geologicznej Polski w skali 1: 50 000, ark. Słupia Nowa [*In Polish*], pp. 1-73. *Wydawnictwa Geologiczne*; Warszawa.

— 1969. Objaśnienia do Szczegółowej mapy geologicznej Polski w skali 1: 50 000, ark. Daleszyce, pp 1-77. *Wydawnictwa Geologiczne*; Warszawa.

— 1980. Objaśnienia do mapy geologicznej Polski 1: 200 000, ark. Kielce, pp. 3-143. *Wydawnictwa Geologiczne*; Warszawa.

FOLK, R.L. 1965. Some aspects of recrystalization in ancient

limestones. *In*: L.C. PRAY & R.C. MURRAY (*Eds*), Dolomitization and limestone diagenesis. *Special Publication Society of Economic Paleontologists and Mineralogists*, **13**, 14-48. Tulsa.

— 1993. SEM imaging of bacteria and nannobacteria in carbonate sediments and rocks. *Journal of Sedimentary Petrology*, **63**, 990-999.

— 1999. Nannobacteria and the precipitation of carbonate in unusual environments. *Sedimentary Geology*, **126**, 47-55.

FOLK, R.L., CHAFETZ, H.S. & TIEZZI, P.A. 1985. Bizarre forms of depositional calcite in hot-spring travertines, central Italy. *In*: N. SCHNEIDERMANN & P.M. HARRIS (*Eds*), Carbonate Cements. *Special Publication Society of Economic Paleontologists and Mineralogists*, **36**, 349-369. Tulsa.

FOLK, R.L. & LYNCH, F.L. 2001. Organic matter, putative nannobacteria and the formation of ooids and hardgrounds. *Sedimentology*, **48**, 215-229.

FORD, T.D. & PEDLEY, H.M. 1996. A review of tufa and travertine deposits of the world. *Earth-Science Reviews*, **41**, 117-175.

GÓRKA, P. 2002. Identyfikacja i modelowanie obiektów dynamicznych dla potrzeb badań geologicznych. MSc Thesis. *Silesian Technical University Arch.*, 120 pp.

GRADZIŃSKI, R. & RADOMSKI, A. 1957. Cavern deposits of „rock milk" in the Szczelina Chochołowska Cave. *Annales Societatis Geologorum Poloniae*, **24**, 63-90. [*In Polish with English summary*]

GRUSZCZYŃSKI, M. & MASTELLA, L. 1986. Calcareous tufas in the area of the Mszana Dolna tectonic window. *Annales Societatis Geologorum Poloniae*, **56**, 117-131. [*In Polish with English summary*]

HALICKI, B. & LILPOP, J. 1932. Czwartorzędowe trawertyny w Gliczarowie i na Podhalu. *Posiedzenia Naukowe PIG*, **33**, 97-98.

HANCOCK, P.L., CHALMERS, R.M.L., ALTUNEL, E. & CAKIR, Z. 1999. Travitonics: using travertines in active fault studies. *Journal of Structural Geology*, **21**, 903-916.

HEM, J.D. 1963. Chemical equillibria and rates of manganese oxidation. *United States Geological Survey Water-Supply Paper*, **1667-A**, 64pp.

— 1964. Deposition and dissolution of manganese oxides. *United States Geological Survey Water-Supply Paper*, **1667-B**, 42pp.

HERCMAN, H. & DEBAENE, G. 2003. Bootstrap and randomisation as a nonparametric methods of accuracy estimation on isochrons method. Climate changes: the karst record III, 3rd Intern. Conf., Montpellier, France, pp. 81-82.

HOEFS, J. 1997. Stable Isotope Geochemistry (4th ed.), 201 pp. *Springer*; Berlin.

ICHIKUNI, M. 1973. Partition of strontium between calcite and solution: effect of substitution of manganese. *Chemical Geology*, **11**, 315-319.

IRWIN, H., CURTIS, C. & COLEMAN, M.L. 1977. Isotopic evidence for source of diagenetic carbonates formed during burial of organic-rich sediments. *Nature*, **269**, 209-213.

IVANOVICH, M. & HARMON, R.S. 1992. Uranium Series Disequilibrium. Applications to environmental problems, 571 pp. *Clarendon*; Oxford.

JANCZEWSKI, E. 1932. Ruchy sejsmiczne zauważone w Polsce w lutym. 1932 r. *Posiedzenia Naukowe PIG*, **33**, 70-72.

JANSSEN, A., SWENNEN, R., PODOOR, N. & KEPPENS, E. 1999. Biological and diagenetic influence in Recent and fossil tufa deposits from Belgium. *Sedimentary Geology*, **126**, 75-95.

KIRKLAND, B.L., LYNCH, F.L., RAHNIS, M.A., FOLK, R.L., MOLINEUX, I.J. & MCLEAN, R.J.C. 1999. Alternative origins for nanno-bacteria-like objects in geology. *Geology*, **27**, 347-350.

KOWALCZEWSKI, Z. & DADLEZ, R. 1996. Tectonics of the Cambrian in the Wiśniówka area (Holy Cross Mts., Central Poland). *Geological Quarterly*, **40**, 23-46.

KOWALSKI, B. 1998. Geologiczne i krajobrazowe konsekwencje poprzecznej dyslokacji łysogórskiej w Górach Świętokrzyskich. *In:* Materiały sesji nt. Przemiany środowiska geograficznego obszarów górskich w Polsce i jego stan współczesny, **II**, pp. 7-16. Kielce.

— 2000. Rzeźba. *In:* S. CIEŚLIŃSKI & A. KOWALKOWSKI (*Eds*), Świętokrzyski Park Narodowy – przyroda, gospodarka, kultura, pp. 107-128. Bodzentyn - Kraków.

— 2002. Geneza układu sieci rzecznej w Górach Świętokrzyskich. *Prace Instytutu Geografii Akademii Świętokrzyskiej w Kielcach*, **7**, 315-351.

KRUMBEIN, W.E. 1979. Calcification by bacteria and algae. *In:* P.A. TRUDINGER & D.J. SWAINE, (*Eds*), Biogeochemical Cycling of Mineralforming Elements, pp. 47-68. *Elsevier* ; New York.

LOISY, C., VERRECHIA, E.P. & DUFOUR, P. 1999. Microbial origin for pedogenic micrite associated with a carbonate palaeosol (Champagne, France). *Sedimentary Geology*, **126**, 193-204.

MARSHALL, K.C. 1979. Biogeochemistry of manganese minerals. *In:* P.A. TRUDINGER & D.J. SWAINE, (*Eds*), Biogeochemical Cycling of Mineralforming Elements, pp. 253-292. *Elsevier*; New York.

MASTELLA, L. 2001. Tektoniczne uwarunkowania występowania martwic wapiennych we fliszu podhalańskim. *In:* Materiały IV. Ogólnopolskiej Konferencji: Neotektonika Polski. Neotektonika, morfotektonika, sejsmotektonika – stan badań i perspektywy rozwoju, pp. 66-79. *Komisja Neotekteniki Komitetu Badań Czwartorzędu PAN*; Kraków.

MASTELLA, L. & MIZERSKI, W. 2002. Budowa geologiczna jednostki łysogórskiej (Góry Świętokrzyskie) na podstawie analizy zdjęć radarowych . *Przegląd Geologiczny*, **50**, 767-772.

MIZERSKI, W. 1978. O zrzutowym charakterze uskoku łysogórskiego. *Biuletyn Geologiczny Uniwersytetu Warszawskiego*, **27**, 193-202.

— 1995. Geotectonic evolution of the Holy Cross Mts. in cen-

tral Europe. *Biuletyn Państwowego Instytutu Geologicznego*, **372**, 1-47.

— 2000. Tektonika i tektogeneza paleozoiku świętokrzyskiego. *Prace Instytutu Geografii Wyższej Szkoły Pedagogicznej w Kielcach*, **4**, 93-125.

MOROZEWICZ, J. 1907. Przyczynki do znajomości węglanu wapniowego. *Kosmos*, **32**, 487-495.

MOUNT, J.F. & COHEN, A.S. 1984. Petrology and geochemistry of rhizolits from Plio-Pleistocene fluvial and marginal lacustrine deposits, East Lake Turkana, Kenya. *Journal of Sedimentary Petrology*, **54**, 263-275.

O'NEIL, J.R. & BARNES, I. 1971. ^{13}C and ^{18}O compositions in some fresh-water carbonates associated with ultramamafic rocks and serpentinites: western United States. *Geochimica et Cosmochimica Acta*, **35**, 687-697.

PEDLEY, M. 2000. Ambient temperature freshwater microbial tufas. *In*: R.E. RIDING & S.M. AWRAMIK (*Eds*), Microbial Sediments, pp. 179-186. *Springer*; Berlin – Heidelberg – New York.

PENTECOST, A. 1993. British travertines: a review. *Proceedings of Geologists' Association*, **104**, 23-39.

— 1995. Quaternary travertine deposits of Europe and Asia Minor. *Quaternary Science Reveiws*, **14**, 1005-1028.

PENTECOST, A. & VILES, H. 1994. A review and reassessment of travertine classification. *Geographie physique et Quaternaire*, **48**, 305-314.

PRZYBYŁOWICZ, W., SCHWARCZ, H.P. & LATHAM, A.G. 1991. Dirty calcites; 2, Uranium-series dating of artificial calcite-detritus mixtures. *Chemical Geology*, **86**, 161-178.

ROMANEK & ZŁONKIEWICZ 1992. Mapa geologiczna podstawowa 1 : 50 000 ark. 817 Nowa Słupia. B – Mapa bez utworów czwartorzędowych. *In*: Mapa geologiczna Polski 1:200 000 ark. Sandomierz. *Państwowy Instytut Geologiczny*; Warszawa.

SANDERS, J.E & FRIEDMAN, G.M. 1967. Origin and occurrence of limestones. *In*: G. V. CHILLINGAR, H.J. BISSEL & R.W. FAIRBRIDGE (*Eds*), Carbonate Rocks, pp. 169-265. *Developments in Sediemntology*, **9A**, *Elvieser*; Amsterdam.

STOOPS, G. 1976. On the nature of "lublinite" from Hollanta (Turkey). *American Mineralogist*, **61**, 172.

STUMM, W. & MORGAN, J.J. 1970. Aquatic Chemistry, 689 pp. *Wiley*; New York.

STUPNICKA, E. & STEMPIEŃ-SAŁEK, M. 2001. Poznajemy Góry Swiętokrzyskie, 173 pp. *Państwowe Wydawnictwo Naukowe*; Warszawa.

SZULC J. 1983. Geneza i klasyfikacja wapiennych osadów martwicowych. *Przegląd Geologiczny*, **31**, 231-236.

TURI, B. 1986. Stable isotopic geochemistry of travertines. *In*: P. FRITZ & J.C. FONTES (*Eds*), Handbook of Environmental Isotope Geochemistry, pp. 207-238. *Elsevier*; Amsterdam.

ZNOSKO, J. 1995. Jeszcze raz o budowie geologicznej Góry Wiśniówki (Góry Świętokrzyskie). *Przegląd Geologiczny*, **43**, 1049-1051.

ZAVARZIN, G.A. 1961. Symbiotic culture of a new microorganism oxidizing manganese. *Microbiology*, **30**, 343-345.

— 1963. Structure of *Metallogenium*. *Microbiology*, **32**, 864-867

Manuscript submitted: 10th May 2003
Revised version accepted: 20th November 2003